5-2024

Investigating Thin Filament Assembly in C. elegans Muscles

Angela Russ

Investigating thin filament assembly in *C. elegans* muscles.

By:

Angela Russ

A thesis submitted in partial fulfillment of the requirements of the Honors College at University of South Alabama and the Bachelor of Sciences in the MABE Department.

University of South Alabama

Mobile

May 2024

Approved by:

Mentor: Ryan Littlefield, PhD

Honors College Representative

David A. Nelson

Digitally signed by David A. Nelson
Date: 2024.05.05 21:35:44 -05'00'

Thesis Committee: David Nelson, PhD

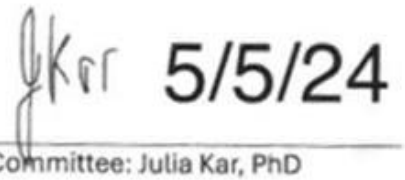

Thesis Committee: Julia Kar, PhD

5/6/2024

Thesis Committee: Joseph Richardson, PhD

Acknowledgements

I would like to thank the imaging lab at the Frederick P. Whiddon College of Medicine, the spring Biology 321 class of 2023, and my fellow undergraduate researchers in Dr. Littlefield's muscle biology lab for helping to make this thesis possible.

Table of Contents

Table of Figures

Table of Tables

Table 1: Common abbreviations and their meanings.

Tmod	Tropomodulin
MhcA	Myosin heavy chain type A
MhcB	Myosin heavy chain type B
myo-3	The gene that regulated mhcA
ng-GFP	Neon green green fluorescent protein
mCH	monomeric Cherry (red fluorescent protein)

Abstract

All striated muscles are composed of small units called sarcomeres [1]. Within each sarcomere, there are thin filaments composed of actin and thick filaments composed of myosin. The thin filaments extend from either end of the thick filament towards the middle of the sarcomere. The lengths of thin filaments are correlated to muscle contraction and force production [1], but it is currently unknown what regulates their lengths. Prior hypotheses based on vertebrate models have focused on a nebulin ruler model [2]. However, nebulin is not present within invertebrate muscles, and this has led to a major gap in the field's knowledge of length regulation. A proposed model of regulation is that the thin filament length is at least partially affected by the myosin in the thick filament chains [3]. To test this model, I made two strains of transgenic *C. elegans* roundworms. Both strains had the Tmod-capped pointed ends of the thin filaments tagged with ng-GFP, and one of them also had a headless *myo-3* mutation marked with mCh. I imaged the strains with a confocal and Nikon Airyscan microscope to determine whether the targeted muscle proteins were visible. The results of these images and genotyping analysis show that the methods used were successful in making the desired model. The images also indicate that the myosin model of thin filament length regulation warrants further investigation.

Background and Introduction

Muscle Physiology

Striated muscles, regardless of type or animal species, are made of small sarcomere units that generate force and contract by shortening. Within these sarcomeres, there are thin filaments containing actin that surround and overlap thick filaments that contain myosin [1]. The thin filaments are also capped at their pointed ends by tropomodulin proteins (Tmod) [1].

Myosin heavy chain (Mhc) is a motor protein that consists of a long tail region and a head domain that binds to and moves along actin filaments. In striated muscle, the myosin heads within the thick filament are organized in a bipolar orientation (Fig. 1). The symmetric orientation means that contractile forces are formed as the myosin motors pull on the thin filaments towards the center of the sarcomere.

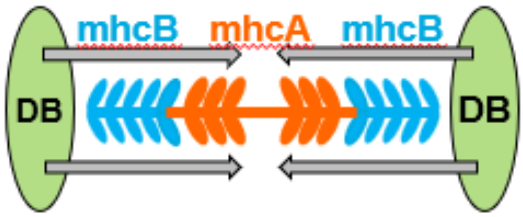

Figure 1. Simplified physiology of a *c. elegans* myofibril.
The thin filaments (grey arrows) start at specialized cells called dense bodies (DB) and grow towards the center of the myofibril where MhcA is located (orange). MhcB (blue) is located on the ends of the myofibril. [4]

Depending on the amount of contraction, the thin filament pointed ends will either overlap, meet, or have a small gap in the middle of the sarcomere. Regardless of overlap, the Tmod-capped pointed ends will be located near the middle of the heavy chain. With a uniform length of the myosin heavy chain, a change in size of the gap between the pointed ends will indicate that the thin filaments have either elongated or shortened.

Muscle Assembly and Regulation

Thin filaments play a key role in muscle contraction, and therefore, force production [1]. The length of the thin filaments specifically can be correlated to the force output of muscles. In vertebrates, the protein nebulin is interwoven with the actin thin filaments [2]. Prior testing showed that nebulin can be a factor that determines thin filament length [1, 2], and the prevailing hypothesis of length regulation points to nebulin as the primary factor in thin filament length regulation [2].

However, recent testing has shown that nebulin only spans 95% of thin filament length [1]. There is also no molecule which plays a similar role to nebulin in invertebrate muscles [3]. Because invertebrate muscles evolved first, and then were slightly modified over time to form vertebrate muscle, it can be inferred that the invertebrate model of thin filament regulation was originally present in vertebrate muscles but now be joined by nebulin.

Recent publications have shown that myosin can be a factor in determining thin filament length in addition to nebulin [3]. Studies involving fruit flies [4], cardiac muscles [6], and striated muscle [7] have shown that thin filament organization and force production is altered when myosin mutations or mutations that affect the binding of thin filaments to myosin heads are present. Researchers have also determined the molecular mechanism by which thin filaments can attach to the heads of myosin chains, and disorders in the production of molecules that bring them together will cause problems with force production and muscle usage [8]. These studies suggested that there is a link

between myosin and thin filament length, but the studies were not able to draw direct comparisons to myosin heads and thin filament length due to other variables being tested.

Testing is further complicated by the composition of the thick filaments in most animal models. Thick filaments are typically composed of one myosin gene, so that many Mhc mutations that disrupt the interaction between the myosin heads and the thin filaments are lethal because they prevent any contraction in the animal model during development. However, *C. elegans* roundworms, which are commonly used as a developmental model for animals, have exceptional muscles because most of their thick filaments are composed of two myosin heavy chains – MhcA and MhcB, each encoded by distinct genes – myo-3 and unc-54, respectively. This physiology allows me to use *C. elegans* as a model to investigate the effect of myosin mutations on the regulation of thin filament lengths.

C. elegans Physiology

C. elegans are semi-transparent roundworms that are commonly used in gene editing models. Their transparency allows for their internal organs and muscles to be imaged with light microscopy as well as image slicing techniques. There are three main types of muscle in adult *C. elegans* hermaphrodites (the common sexual form in this species). Body wall muscle (BWM) runs the length of the worm in two stripes along its body. It is located on the outside of the worm, allowing for an unobstructed view of the BWM oblique striations. The vulva muscle (VM) and anal depressor muscle (ADM) are also easily seen with common microscopy techniques (Fig. 2). The thick filaments in each of these muscles are composed of two myosin isoforms. The middle of the thick filament is composed of myosin A (MhcA), and on either end by myosin B (MhcB) [4]. The thin filaments start on either end of the thick filament and go towards the middle over the MhcA region (Fig.1).

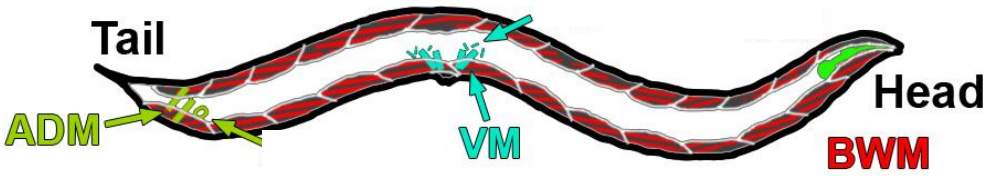

Figure 2. Simplified physiology of *C. elegans* muscles.
Body muscle types of adult *C. elegans* hermaphrodites. Key types are the body wall muscle (BWM), vulva muscle (VM), and anal depressor muscle (ADM).

Most *C. elegans* are hermaphrodites that reproduce by self-mating and typically maintained in the lab as purebred strains, in that all of the genes are homozygous and the progeny are clonal. However, hybrid strains can be generated using *C. elegans* males, which are naturally present at low frequency, and can be mated with hermaphrodites from other strains. The progeny of this mating would have one chromosome copy from the hermaphrodite and one copy from the male, so they would have a 50% chance of being a male. The *unc-94* gene that encodes Tmod is located on chromosome I and the *myo-3* gene that encodes MhcA is located on chromosome V.

CRISPR-Cas9

CRISPR-Cas9 is a technique that uses the Cas9 protein to cut DNA at a specific location [9]. A strand of guide RNA (sgRNA) associates with Cas9 and targets it to a unique gene sequence. The Cas9-sgRNA complex allows researchers to cut at specific genes that are near a CRISPR cut site. The *unc-94* and *myo-3* genes are ideal targets for gene editing as they have CRISPR cut sites near the genes that control aspects of their expression. Once the chromosomal DNA is cut by the Cas9-sgRNA complex, the cell initiates a repair process, in which similar (homologous) sequences are used to rejoin the chromosome fragments [10, 11]. Through this process of homology directed repair, a donor molecule can provide the sequence for the repair allowing researchers to insert additional genetic material at a specific genetic location.

Project Question and Hypothesis

There are several disorders which impact muscle function in all species, including muscular dystrophies, but little is known about the physiology behind them. Without knowing how the thin filament length is determined, it is impossible to know if that mechanism is the cause of these disorders and how to treat them. The model of thin filament length regulation can be developed to answer other questions in this field.

The structure of the thick and thin filaments within sarcomeres suggests a model of thin filament length regulation based on the myosin head regions, where the thin filaments rely on the presence of myosin heads to grow and extend. In this model, the thin filaments can be seen as a vine, and the myosin is a rod the vine grows along. The vine will only be able to grow as high as the rod is, and in muscles the thin filaments can only grow until they run out of myosin heads to which they attach.

To test this model of regulation, the myosin heads in the mhcA region need to be removed, and the Tmod located at the pointed ends of the thin filaments needs to be marked. Disruptions in thin filament regulation can be found by comparing a control strain of worms that have only their Tmod marked to a hybrid strain that has marked Tmod and the mhcA heads removed. The differences in the thin filament between these two strains will indicate whether myosin has an effect on thin filament length regulation (Fig.3).

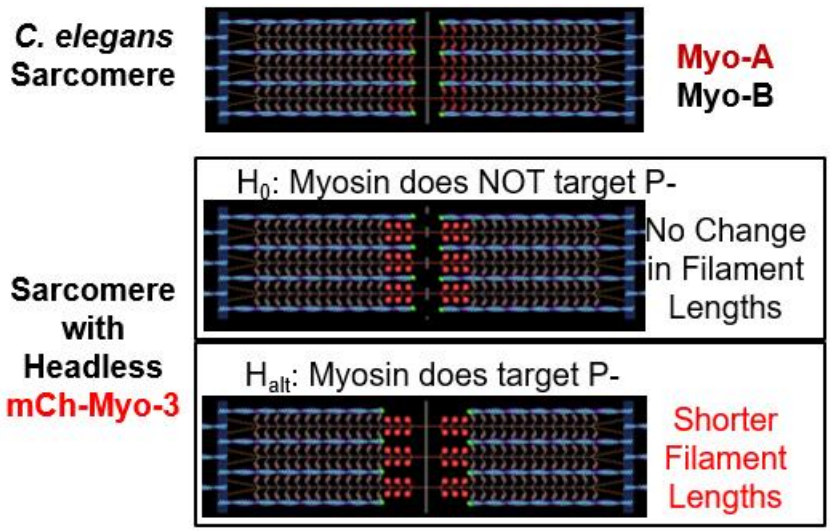

Figure 3. Null and alternate hypotheses of the myosin model of thin filament regulation.
The null hypothesis (H_0) states that there will be no change in thin filament lengths if the heads of the myo-3 are removed, and the alternate hypothesis (H_{alt}) states that the thin filaments will shorten without myo-A heads.

It is expected that the removal of myosin heads from the mhcA region will result in shorter thin filament lengths (Fig. 3). This change will be visible in *C. elegans* muscles as changes in their oblique striations of the BWM, as well as changes in their ADM and VM. In the BWM, it is expected that there will be visible separations or gaps in some of the striations, as well as small segments of striations that are separate from the larger striations.

Methodology

Two genetic edits were selected to mark the thin filaments in the BWM of *C. elegans* for analysis. The first edit tagged the Tmod pointed ends with neon green fluorescent protein (ng-GFP). The second edit removed the myosin heads in the myo-A section of the heavy chain (gene myo-3) and replaced them with the neon red fluorescent protein mCherry (mCh). The strain containing the mCh headless myosin had already been created and named RSL6. The process of making the genetic insert for ng-GFP Tmod used a plasmid named PDD400 (Fig. 4).

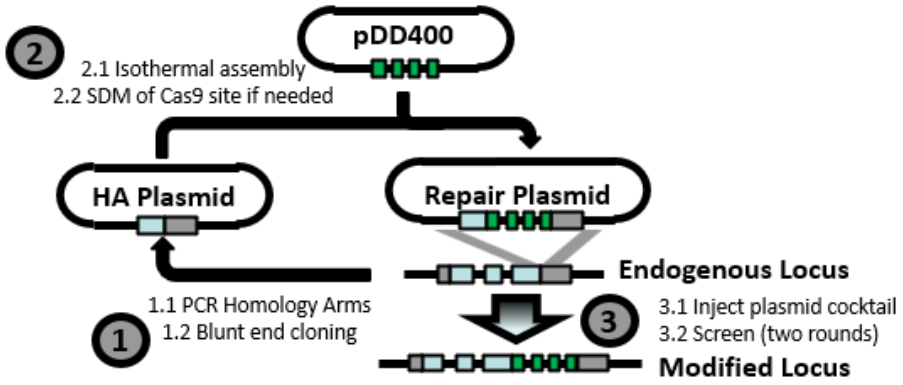

Figure 4. Process of making repair plasmid for ng-GFP.
The process of generating a repair plasmid and genetic insert for ng-GFP is shown using the plasmid pDD400.

An additional genetic edit was selected to help locate worms whose genes were affected by the CRISPR-CAS9 injection. This edit inserts the *rol-6* gene and creates “roller”

worms that move in a corkscrew motion. This mutation makes edited worms easy to see when they are on the same plate as unedited worms that move sinusoidally (Fig. 5).

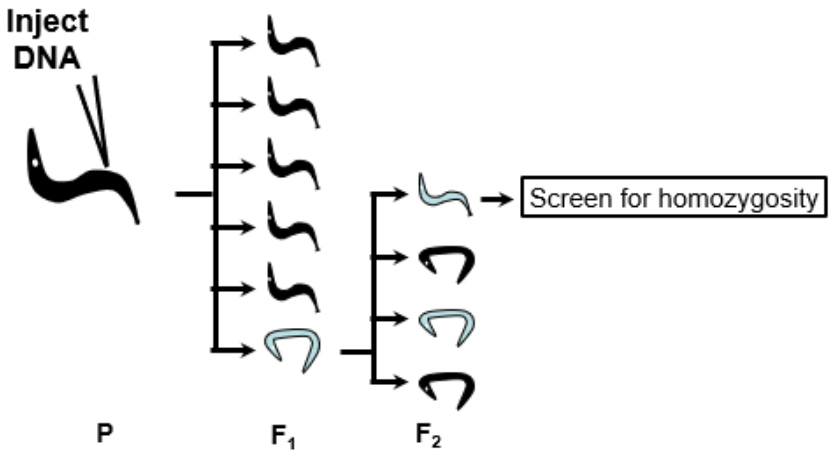

Figure 5. Standard screening process for transgenic progeny.
The standard screening process involves selecting roller worms from the first generation (F1) and then screening fluorescent progeny of the second generation (F2) for homozygosity. [8]

To make the transgenic strain with ng-GFP Tmod, fifteen worms were selected at the stage of their lifecycle where they were forming eggs inside of their body. An injection mix was then made of 0.7 µl nuclease-free water, 6.5 µl of the ng-GFP donor molecule at a concentration of 150 ng/µl, 1.0 µl of CAS-9 at 20 µM concentration, and 0.5 µl of ng-GFP guide RNA at 100 µM. The mix also contained 0.3 µl of guide *rol-6* guide RNA at 100 µM and 1.0 µl of rol-6 donor molecule. This mix was then injected into the somatic gonads of the fifteen worms, targeting the genetic material in their gonads that would be placed into eggs.

From there, five sets of three worms were set onto plates numbered 1 – 5 A. The worms remained on those plates for 12 hours, and then the worms were moved onto a new set of plates labelled 1 – 5 B. After 24 hours, they were moved again to plates 1 – 5 C. This

was done to estimate which eggs were formed at specific times in the gonads of the parent worms. For the first 12 hours, it was likely that the eggs being laid had been formed in the parent worms before they were injected. After the next 24 hours it was likely that the worms would have no new eggs formed. The C plate was used since the exact age of the worms could not be known, and some would still be laying eggs 36 hours after injection if they were younger than predicted.

The fifteen plates made from this process were then screened for rolling progeny (Fig. 5). A "roller" that was observed was then placed onto a separate plate and allowed to reproduce by itself. These plates were numbered according to the plate line from which the roller was pulled, with a roller from the number 1 line named 1xx, from the number 2 line named 2xx, and so on. The progeny of this self-replication was then screened for ng-GFP using fluorescent microscopy (Fig. 5). If all worms screened from a plate contained ng-GFP, it was likely that the worms on that plate were homozygous for the ng-GFP edit.

Three homozygous plates were identified with this process: AR323, AR415, and AR519. These plates were also further refined by carrying only non-rolling progeny onto new plates, so that the *rol-6* gene was eventually removed from the populations' genotypes. The genotypes of the three strains were verified by visual inspection for fluorescence, PCR genotyping, and genetic sequencing. Strain AR415 was renamed RSL119.

Unedited worms were placed onto an empty plate and "heat shocked" at 30˚C for four hours to make unedited male worms. Eight of these males were placed on a plate with three hermaphrodites of the RSL 6 line. Their progeny was screened to find males with red

fluorescence, as the only way a male could have that fluorescence was if it was progeny from RSL6 and the unedited males. It was expected that the progeny males would have one copy of the mCh headless myosin and one unedited chromosome.

Worms were selected from each of the homozygous ng-GFP plates and placed onto new plates in groups of three. Red fluorescing males were then added to these new plates in groups of eight to interbreed. The progeny from this mating were screened for red fluorescing hermaphrodites and put onto empty plates alone. It was expected that a red hermaphrodite would be the progeny of the ng-GFP hermaphrodites and red males, and that they would have one copy of each edited chromosome.

The progeny of their self-crossing was screened for red and green fluorescence until a strain was found that was homozygous for both edits. This strain was named RSL122.

RSL119 and RSL122 were imaged using a confocal and Nikon Airyscan microscope. The worms were immobilized using the paralytic drug muscimol, which does not contract the worms' muscles. The strains were imaged using vertical slices to form a depth-coded image on the Airyscan and confocal microscopes.

Results

Three strains were identified to be homozygous for the ng-GFP edit that originated from separate injection groups (AR323, AR415, and AR525). It was confirmed using visual inspection and PCR genotyping that RSL119 and RSL122 were homozygous for ng-GFP Tmod and headless mCh myo-3. RSL119 was further confirmed to be homozygous for the ng-GFP edit using gene sequencing.

Table 2: Transgenic strains generated in this thesis.

Strain Name / Number	**Genetic Tagging**
AR323 AR415 (Renamed RSL119) AR525	Ng-GFP tagged to Tmod on thin filament pointed ends
RSL122	mCH replacing myosin heads in the mhcA region of thick filament

The images taken of RSL119 show the localization of Tmod and its tagged ng-GFP to the pointed ends of the thin filaments (Fig. 6). The localization of ng-GFP tagged Tmod was also seen in the ADM using depth-coded imaging (Fig.7) such that the vertical distance between the muscles was visible. The images show the typical localization of Tmod in *C. elegans* with unedited myosin chains. These images are displayed in greyscale to achieve a higher resolution.

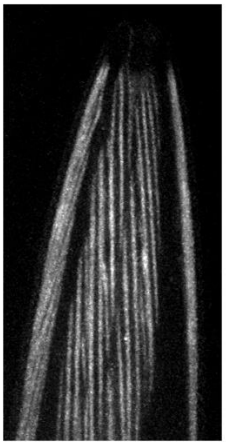

Figure 6. Tmod localization in BWM. The ng-GFP Tmod is seen localizing in distinct striations in the BWM of the *C. elegans* head region.

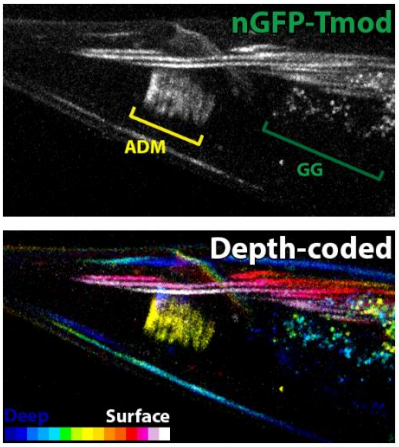

Figure 7. Tmod localization in ADM. The ng-GFP Tmod is seen localizing in the BWM and ADM of *C. elegans* (top). The depth-coded image (bottom) shows the distance between BWM and ADM. Gut granules are visible in the top image.

The images of RSL122 show the localization of ng-GFP Tmod to the same areas as was observed in RSL119 and distinct striations of the headless mCh-myo-3 (Fig. 8). The overlay image (Fig. 9) shows the orientation of the headless mCh-myo-3 sections and the ng-GFP Tmod relative to one another. This image is shown in its original colors to tell the fluorescent markers apart. The ng-GFP Tmod and headless mCh-myo-3 were also visible in *C. elegans* embryos (Fig. 10), where no distinct striations were visible.

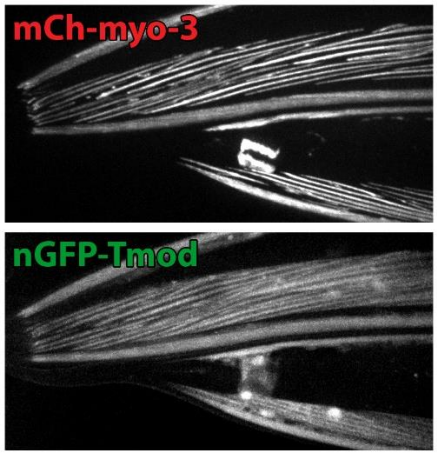

Figure 8. Two fluorescent markers visible in RSL 122.
The headless mCh myo-3 (top) is seen forming distinct striations in the BWM with ng-GFP Tmod (bottom).

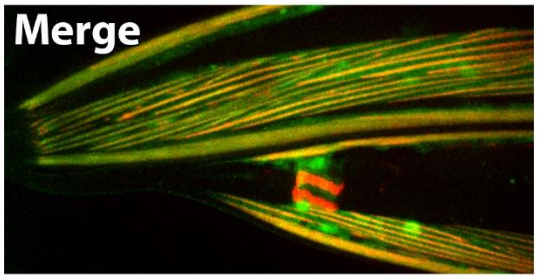

Figure 9. Overlay image of fluorescent markers in RSL 122.
The ng-GFP Tmod (green) is seen forming striations alongside the headless myo-3 (red) in *C. elegans* BWM.

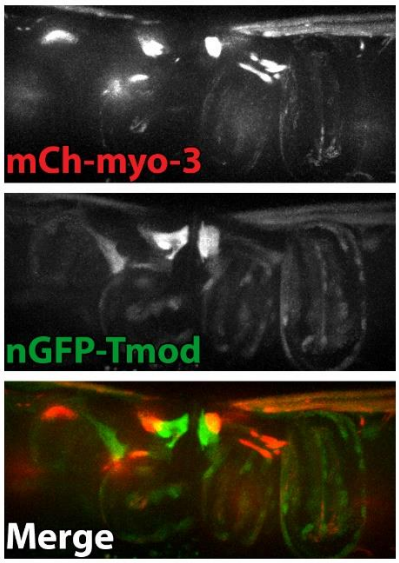

Figure 10. Two fluorescent markers and overlay in *C. elegans* embryos.
Headless mCh myo-3 (top) and ng-GFP Tmod (middle) are visible in *C. elegans* eggs through the body of the mother worm. The overlay image (bottom) shows their orientation and the bright VM of the mother worm.

Discussion

The images taken of RSL119 show the normal localization of ng-GFP Tmod when the myosin chains are not altered. The head region of RSL119 had a few visible spots where a striation widened (Fig. 6). The depth-coded image shows the orientation of Tmod as it is expressed within *C. elegans* bodies, and it also indicates that distinct striations are not as visible in the ADM and as the BWM (Fig. 6).

The images of RSL122 show the distinct striations of the headless mCh-myo-3 and the ng-GFP localizing near it. While both fluorescent markers are visible in the *C. elegans* embryos, significantly less myo-3 is formed in them than the Tmod at that stage of development (Fig. 10). The Tmod is not seen forming distinct striations in the embryos, indicating that the regulating mechanism was not yet present in the embryos. Additionally, there are locations in the head region of RSL122, which appear to be Tmod striations separating from one another or having a shorter length than expected (Fig. 8), which would indicate a shift in the regulatory mechanism from RSL119.

The images taken of RSL119 and RSL122 validate the injection and mating scheme used to produce the two strains. Two novel transgenic strains were successfully created and imaged using this process, and the two fluorescent markers were distinctly visible using vertical imaging techniques. The analysis of the images provides preliminary results which indicate a shift in the regulatory mechanism of thin filaments in *C. elegans*. The presence of more Tmod striation separations and shorter lengths in RSL122 (Fig. 8), as well

as the lack of Tmod striations in *C. elegans* embryos when *myo-3* is not fully expressed (Fig. 10) further indicate that *myo-3* may have a role in thin filament regulation.

However, higher resolution images are needed to provide more conclusive evidence towards the myosin model of thin filament regulation. Images comparing the striations in *C. elegans* embryos with and without the headless mCh-myo-3, as well as a larger sample size of images, would be a key next step in investigating this regulation model further. The analysis of the images of RSL119 and RSL122 indicate that there is merit to the myosin model of thin filament regulation, and that further tests are warranted to understand the extent to which myosin affects the thin filaments.

The results demonstrate that this methodology successfully creates two novel nematode models for studying thin filament regulation and how it is impacted by myosin. The visual inspection, PCR genotyping, and genetic sequencing results show that the methodology used in this thesis is a viable model for remaking these animal models. Additionally, the preliminary results of the image analysis indicate that further research is warranted into the myosin model of thin filament regulation.

References

[1] Szikora, S., Görög, P., & Mihály, J. (2022). The mechanisms of thin filament assembly and length regulation in muscles. International Journal of Molecular Sciences, 23(10), 53065331. https://doi.org/10.3390/ijms23105306

[2] Chu M, Gregorio CC, Pappas CT. Nebulin, a multi-functional giant. J Exp Biol. 2016 Jan;219(Pt 2):146-52. doi: 10.1242/jeb.126383. PMID: 26792324; PMCID: PMC6514474.

[3] Littlefield RS, Fowler VM. Thin filament length regulation in striated muscle sarcomeres: pointed-end dynamics go beyond a nebulin ruler. Semin Cell Dev Biol. 2008 Dec;19(6):511-9. doi: 10.1016/j.semcdb.2008.08.009. Epub 2008 Aug 26. PMID: 18793739; PMCID: PMC2650474.

[4] Miller, D. M. III, Ortiz, I., Berliner, G. C., and H. F. Epstein. (1983). Differential localization of two myosins within nematode thick filaments. Cell, 34(2).

[5] Chun, M., & Falkenthal, S. (1988). IFM(2)2 is a myosin heavy chain allele that disrupts myofibrillar assembly only in the indirect flight muscle of drosophila melanogaster. Journal of Cell Biology, 107(6), 2613–2621. https://doi.org/10.1083/jcb.107.6.2613

[6] Latham, S. L., Weiß, N., Schwanke, K., Thiel, C., Croucher, D. R., Zweigerdt, R., Manstein, D. J., & Taft, M. H. (2020). Myosin-18B regulates higher-order organization of the cardiac sarcomere through thin filament cross-linking and thick filament dynamics. Cell Reports, 32(9), 108090. https://doi.org/10.1016/j.celrep.2020.108090

[7] Robaszkiewicz, K., Śliwinska, M., & Moraczewska, J. (2020). Regulation of actin filament length by muscle isoforms of tropomyosin and Cofilin. International Journal of Molecular Sciences, 21(12), 4285. https://doi.org/10.3390/ijms21124285

[8] McArdle, K., Allen, T. S. C., & Bucher, E. A. (1998). Ca2+-dependent muscle dysfunction caused by mutation of the Caenorhabditis elegans troponin T-1 gene. Journal of Cell Biology, 143(5), 1201–1213. https://doi.org/10.1083/jcb.143.5.1201

[9] Redman M, King A, Watson C, King D. (2016) What is CRISPR/Cas9? National Institute of Health., 101(4), 213-5. doi: 10.1136/archdischild-2016-310459. PMID: 27059283; PMCID: PMC4975809.

[7.510] Dickinson DJ, Ward JD, Reiner DJ, Goldstein B. Engineering the Caenorhabditis elegans genome using Cas9-triggered homologous recombination. Nat Methods. 2013 Oct;10(10):1028-34. doi: 10.1038/nmeth.2641. Epub 2013 Sep 1. PMID: 23995389; PMCID: PMC3905680.

[11] J. A. Arribere, R. T. Bell, B. X. Fu, K. L. Artiles, P. S. Hartman, A. Z. Fire. (2014). Efficient marker-free recovery of custom genetic modification with CRISPR/CAS9 in Caenorhabditis elegans. Genetics, 198 pp. 837-846